Atmos. Meas. Tech. Discuss., 8, 12025–12050, 2015
www.atmos-meas-tech-discuss.net/8/12025/2015/
doi:10.5194/amtd-8-12025-2015

Atmospheric Measurement Techniques Discussions
Open Access

Measuring morphology and density of internally mixed black carbon with SP2 and VTDMA: new insight to absorption enhancement of black carbon in the atmosphere

Y. X. Zhang[1], Q. Zhang[1,6], Y. F. Cheng[2], H. Su[2], S. Kecorius[3], Z. B. Wang[3,2], Z. J. Wu[4,3], M. Hu[4,6], T. Zhu[4,6], A. Wiedensohler[3], and K. B. He[5,6]

[1]Ministry of Education Key Laboratory for Earth System Modeling, Center for Earth System Science, Tsinghua University, Beijing 100084, China
[2]Multiphase Chemistry Department, Max Planck Institute for Chemistry, 55020 Mainz, Germany
[3]Leibniz-Institute for Tropospheric Research, 04318 Leipzig, Germany
[4]State Key Joint Laboratory of Environmental Simulation and Pollution Control, College of Environmental Sciences and Engineering, Peking University, Beijing 100871, China
[5]State Key Joint Laboratory of Environment Simulation and Pollution Control, School of Environment, Tsinghua University, Beijing 100084, China

[6]The Collaborative Innovation Center for Regional Environmental Quality, Beijing 100084, China

Received: 1 October 2015 – Accepted: 4 November 2015 – Published: 18 November 2015

Correspondence to: Q. Zhang (qiangzhang@tsinghua.edu.cn) and H. Su (h.su@mpic.de)

Published by Copernicus Publications on behalf of the European Geosciences Union.

Abstract

The morphology and density of black carbon (BC) cores in internally mixed BC (In-BC) particles affects their mixing state and absorption enhancement. In this work, we developed a new method to measure the morphology and effective density of BC cores of ambient In-BC particles using a single particle soot photometer (SP2) and a volatility tandem differential mobility analyzer (VTDMA), during the CAREBeijing-2013 campaign from 8 to 27 July 2013 at Xianghe Observatory. The new measurement system can select size-resolved ambient In-BC particles and measure the mobility size and mass of In-BC cores. The morphology and effective density of ambient In-BC cores are then calculated. For In-BC cores in the atmosphere, changes in the dynamic shape factor (χ) and effective density (ρ_{eff}) can be characterized as a function of aging process (D_p/D_c) measured by SP2 and VTDMA. During an intensive field study, the ambient In-BC cores had an average χ of ~ 1.2 and an average density of $\sim 1.2\,\text{g cm}^{-3}$, indicating that ambient In-BC cores have a near-spherical shape with an internal void of $\sim 30\,\%$. With the measured morphology and density, the average shell/core ratio and absorption enhancement (E_ab) from ambient black carbon were estimated to be 2.1–2.7 and 1.6–1.9 for different sizes of In-BC particles at 200–350 nm. When assuming the In-BC cores have a void-free BC sphere with a density of $1.8\,\text{g cm}^{-3}$, the shell/core ratio and E_ab could be overestimated by ~ 13 and $\sim 17\,\%$ respectively. The new approach developed in this work will help improve calculations of mixing state and optical properties of ambient In-BC particles by quantification of changes in morphology and density of ambient In-BC cores during aging process.

1 Introduction

The light-absorbing capability of black carbon (BC) particles closely relates to their morphology and density in the atmosphere (Zhang et al., 2008; Rissler et al., 2014). The morphology and density of BC particles is affected by their aging processes (Rissler

et al., 2013; Geller et al., 2006). Fresh or externally mixed BC (Ex-BC) particles close to emission sources exist in fractal-like agglomerates, consisting of small BC spherules with a size of 15–30 nm formed via coagulation processes (Park et al., 2003; Slowik et al., 2004). BC particle then undergoes significant changes in physicochemical characteristics during aging process in the atmosphere, forming the internally mixed BC (In-BC) particle consisting of BC core and coating materials (Cheng et al., 2006). When coated with a non-absorbing shell, void-containing BC particle with open structure transforms into a compact BC core with a near-spherical morphology, less internal voids, and higher density, resulting in a decrease of core size and an increase of refractive index for BC core (Bond and Bergstrom, 2006; Qiu et al., 2012; Khalizov et al., 2013). According to Mie theory, the absorption enhancement of In-BC was depended on its BC core size, coating thickness, and refractive index of both BC core and coatings (Fuller et al., 1999; Bond et al., 2006; Lack and Cappa, 2010). In this regard, understanding the atmospheric evolution of the morphology and density of BC core is important for investigating optical properties of In-BC particles, given that the size and refractive index of BC core are determined by its morphology and density (Adler et al., 2010; Scarnato et al., 2013; Radney et al., 2014).

By now, the absorption enhancement of In-BC particles is still unclear, partly due to lack of understanding on the evolution of morphology and density of BC particles in the atmosphere (Xue et al., 2009a; Knox et al., 2009; Chan et al., 2011; Cappa et al., 2012). Recent in-situ measurements argued that the absorption enhancement of In-BC particles may have been overestimated in previous estimates (Cappa et al., 2012), because they usually treated the In-BC core as spherical with no voids throughout the atmospheric lifetime when calculating absorption enhancement of In-BC particles (Jacobson et al., 2000, 2001; Bond et al., 2006). This improper assumption may lead to significant biases on absorption enhancement estimates by omitting the evolution of morphology and density of BC core during atmospheric aging as well as the impact of aging time to absorption enhancement.

To quantify how the morphology and density changes of BC cores impact the absorption enhancement of ambient In-BC particles, an online measurement system must be developed with the capability that can separate Ex-BC and In-BC particles, because those Ex-BC fractions can induce unpredictable errors when calculating morphology of In-BC cores. The morphology of aerosol particles can be measured by several measurement techniques including transmission electron microscopy (TEM), angular light scattering (ALS), atomic force microscopy (AFM), differential mobility analyzer–electrical low pressure impactors (DMA–ELPI), and a differential mobility analyzer–aerosol particle mass analyzers (DMA–APM) (Köylü et al., 1995; Sgro et al., 2003; Maricq et al., 2004; McMurry et al., 2002). However, none of them can distinguish Ex-BC and In-BC cores in the atmosphere. Changes in core morphology and density of In-BC particles are usually assessed in laboratorial experiments with generated BC cores by mimicking the formation of In-BC particles during atmospheric aging (e.g., Qiu et al., 2012). For example, DMA-APM combined with a heating unit can remove the coating materials of BC-containing particles and estimate the morphology and density BC component by measuring the mobility size and particle mass of BC core (Zhang et al., 2008; Pagels et al., 2009). Because DMA-APM cannot separate the influence from Ex-BC particles, it is only used in laboratory measurements with generated Ex-BC or In-BC particles (McMurry et al., 2002; Xue et al., 2009b).

In this study, we develop a novel method for in-situ measurements of the morphology and effective density of ambient In-BC cores using a volatility tandem differential mobility analyzer (VTDMA) and a single particle soot photometer (SP2). This combined VTDMA-SP2 system provides direct measurement of the mobility size and single particle mass of In-BC cores, which are then used to determine the morphology and effective density. Evolution of morphology and density of ambient In-BC cores during aging process are characterized with the new approach. Finally, absorption enhancement of ambient In-BC aerosols is estimated, taking into core morphology and density into account.

2 Methods and data

2.1 Measurement system

The new measurement system is developed to obtain the morphology, density, mixing state and optical properties of ambient In-BC particles, as shown in Fig. 1. The system is consisted by a VTDMA and a SP2. Ambient aerosols were collected using a sampling system, comprising a PM_{10} cyclone inlet and a silica-gel diffusion dryer system (Tuch et al., 2009).

The VTDMA section, including two differential mobility analyzers (DMA), two condensation particle counters (CPC), and two thermo-denuders, is used to determine the mobility size (D_m) of In-BC cores. The VTDMA method investigates the mixing state of BC particle by measuring the change of aerosol particle size at different temperatures. Specifications for the VTDMA have been documented in previous literatures (Philippin et al., 2004; Wehner et al., 2009; Cheng et al., 2012). Briefly, quasi-monodisperse particles with sizes of 200, 250, 300 and 350 nm are pre-selected using the first DMA (DMA1) and counted with the first CPC (CPC1). These prescribed particles passed through a thermo-denuder at 300 °C (or at 25 °C for the control group), then BC as a refractory component will remain in the particle phase after heating while the rest component tends to evaporate resulting in a change of particle size (Cheng et al., 2009). Therefore, the Ex-BC size has no or slight change, but the In-BC size will be significantly decreased due to the evaporation of coatings. The change is then measured by the second DMA (DMA2) and CPC (CPC2) to discriminate In-BC from Ex-BC and derive the D_m of In-BC cores.

SP2 measurements are used obtain the mass (m) of individual In-BC core and the scattering cross section of individual In-BC particle. Specifications for the SP2 instrument can be found in previous publications (Schwarz et al., 2006; Gao et al., 2007; Sedlacek et al., 2012). SP2 also measures quasi-monodisperse particles selected by the DMA1 in four sizes (200, 250, 300 and 350 nm), recording their incandescent and scattering signals induced by a Nd:YAG intra-cavity laser at 1064 nm. The incandescent light can be produced when refractory BC is heated to more than 4000 °C by absorbing laser light at 1064 nm, thus the mass of BC particle is identified by its incandescent intensity. Furthermore, the In-BC particle can be distinguished using the delay time between the peaks of the scattering and incandescent signals (Sedlacek et al., 2012). In our study, a delay time of 1.6 µs was chosen to discriminate between Ex-BC (< 1.6 µs) and In-BC (≥ 1.6 µs) types, based on the delay time distribution obtained from the SP2 measurements (see Fig. S1 in the Supplement). The mass (m) of individual In-BC core is determined from the incandescent intensities, which is calibrated by the incandescent intensities of Aquadag particles in SP2 (Gysel et al., 2011; Moteki and Kondo, 2010; Baumgardner et al., 2012). Coatings of In-BC particles gradually volatilize through the laser beam due to thermal radiation from BC component, causing the changes in scattering properties of In-BC particles. The initial scattering intensity of individual In-BC particle is derived from the leading-edge-only (LEO) fit (Gao et al., 2007) to determine its scattering cross section (C_s) based on calibration using polystyrene latex spheres (PSL). The validity of LEO fit used for ambient particles is checked in our study (see Fig. S2).

The measurement system was deployed at the Xianghe Atmospheric Observatory (39.80° N, 116.96° E) from 8 to 27 July 2013, as part of CAREBeijing-2013 campaign. The Xianghe site is located in southeast Beijing, northwest of Tianjin. The Xianghe observatory is surrounded by residential areas, about 5 km from the local town center.

2.2 Theoretical calculation

2.2.1 Morphology and effective density

In this study, the morphology of In-BC cores is characterized by particle size (D_m), shape factor (χ), and void ratio (R_{void}) (DeCarlo et al., 2004). Ambient aerosols are usually non-spherical particles (e.g., BC aggregates), as such, their structural parameters are complex. The size of irregular particles is determined as an equivalent diameter, i.e., mobility diameter (D_m) (Khalizov et al., 2013). Meanwhile, the density of the

BC core is characterized by effective density (ρ_{eff}) (Zhang et al., 2008). These above parameters can be calculated as follows.

The ρ_{eff} of the In-BC core is calculated as the ratio of mass (m, fg) from SP2 measurement to D_m from VTDMA measurement, assuming In-BC core as a sphere. Then ρ_{eff} can be written as:

$$\rho_{eff} = \frac{6m}{\pi D_m^3}. \quad (1)$$

The χ of the In-BC core is calculated from D_m and volume equivalent diameter (D_{ve}), as Eq. (2):

$$\chi = \frac{D_m \times C_c(D_{ve})}{D_{ve} \times C_c(D_m)}, \quad (2)$$

where D_{ve} is calculated from the mass of In-BC core measured by SP2 by assuming ρ_{BC} of 1.8 g cm^{-3}; C_c is the Cunningham Slip Correction Factor parameterized as:

$$C_c(D) = 1 + \frac{2\lambda}{D}\left[\alpha + \beta \exp\left(-\frac{\gamma \times D}{2\lambda}\right)\right], \quad (3)$$

where D is the particle size (D_{ve} or D_m) and λ is the mean free path of gas molecules (65 nm used in our study); the empirical constants α, β and γ are respectively 1.142, 0.558 and 0.999 (Allen and Raabe, 1985).

Assuming a spherical core of In-BC particle in this study, R_{void} is calculated by the D_{ve} and D_m of In-BC core, as Eq. (4):

$$R_{void} = 1 - \frac{D_{ve}^3}{D_m^3}. \quad (4)$$

Discussion Paper | Discussion Paper | Discussion Paper | Discussion Paper |

2.2.2 Absorption enhancement

The absorption enhancement (E_{ab}) of In-BC particle is defined as the ratio of the absorption cross section between BC particles covered with coatings ($C_{ab,\,p}$) and bare BC cores ($C_{ab,\,c}$), which is calculated by the core size (D_c), particle size (D_p) and the refractive indices of non-BC coatings (RI_{nonBC}) and BC core (RI_c) using Mie model, as given in Eq. (5):

$$E_{ab} = \frac{C_{ab,\,p}(D_c, D_p, RI_{nonBC}, RI_c)}{C_{ab,\,c}(D_c, RI_c)}. \quad (5)$$

D_c is derived from the mass (m) of In-BC core measured by SP2 and its density (ρ_c). In previous studies, a prescribed ρ_c value of 1.8 g cm^{-3} has been used based on an assumption of void-free spherical core of In-BC particle (Moteki and Kondo, 2010; Cappa et al., 2012). In this work, the ρ_c is characterized by the effective density (ρ_{eff}), taking the morphology (χ and R_{void}) of In-BC core into account. In summary, D_c is calculated by Eq. (6):

$$D_c = \left(\frac{6m}{\pi\rho_c}\right)^{1/3} = \left(\frac{6m}{\pi\rho_{eff}}\right)^{1/3}. \quad (6)$$

D_p is determined by the Mie theory calculation with a shell-and-core mode (Metcalf et al., 2013), relating to C_s, D_c and RI_{nonBC} and RI_c, as shown in Eq. (7):

$$D_P \sim (C_s, D_c, RI_{nonBC}, RI_c), \quad (7)$$

in which C_s is obtained from SP2 scattering signal using LEO fit (Gao et al., 2007); the RI_{nonBC} used in this study is deduced from SP2-VTDMA measurements and Mie theory calculation, which is presented in the Supplement (Fig. S3). Given that voids in In-BC cores can be filled by either air or non-BC components or both, we selected two ideal cases to calculate the RI_c in the following analysis: one is with all voids filled with

air (RI_c(air)), and the other is with all voids filled by non-BC components (RI_c(nonBC)), as Eq. (9):

$$RI_c(\text{air}) = \left[n_{BC} \times (1 - R_{void}) + n_{air} \times R_{void}\right] + \left[k_{BC} \times (1 - R_{void})\right] i, \quad (8)$$

$$RI_c(\text{nonBC}) = \left[n_{BC} \times (1 - R_{void}) + n_{nonBC} \times R_{void}\right] + \left[k_{BC} \times (1 - R_{void})\right] i, \quad (9)$$

where n_{BC}, n_{air} and n_{nonBC} are the real parts of RI for BC materials, air and non-BC components (with $n_{BC} = 1.95$, $n_{air} = 1.0$ and $n_{nonBC} = 1.42$); and k_{BC} is the imaginary part of the refractive index for BC ($k_{BC} = 0.79$) (Bond and Bergstrom, 2006).

3 Results and discussions

3.1 Comparing volume size distribution of In-BC cores measured by VTDMA and SP2

Figure 2 presents the volume size distributions of mixed Ex-BC and In-BC cores measured by VTDMA and In-BC cores measured by SP2 for the four prescribed size ranges through DMA1. After heating to 300 °C, the residual particles measured by VTDMA mainly include both Ex-BC particles and In-BC cores (Philippin et al., 2004; Cheng et al., 2009). Bimodal distribution was observed in VTDMA measurements, representing the size distributions of Ex-BC and In-BC cores respectively. The peaks at initially prescribed size ranges represent Ex-BC particles because they did not undergo a size change after heating. The peaks at smaller size represent the sizes of In-BC cores, which are 154–201 nm smaller than their initial sizes with coatings (200–350 nm).

For SP2 measurements presented in Fig. 2, size of individual In-BC core was calculated by its mass and density of BC (1.8 g cm^{-3}), assuming that In-BC core has a void-free sphere morphology. The peaks in SP2 measured size distributions of In-BC cores were 102–161 nm smaller than their initial sizes, remarkably lower than VTDMA measurements. The large discrepancies between SP2 and VTDMA measurements suggest that the morphology of In-BC cores differed from a void-free spherical shape, because voids in In-BC core have resulted in a lower density and lager size, in which the latter was observed by VTDMA measurements. In this case, the ρ_{BC} of 1.8 $g\,cm^{-3}$ used to calculate the size of BC cores would be inappropriate for SP2 measurements.

3.2 Morphology and effective density of In-BC cores

The size differences of In-BC cores measured by SP2 and VTDMA are then used to derive the morphology and effective density of In-BC cores. For each mobility size of BC particles (200, 250, 300 and 350 nm) presented in Fig. 2, the peak in SP2 measurements and the first peak in VTDMA measurements represent the volume equivalent diameter and the mobility diameter of In-BC cores respectively. The shape factor (χ) and effective density (ρ_{eff}) of In-BC cores are then calculated following Eqs. (1) and (2).

Figure 3 presented the evolution in χ and ρ_{eff} with aging process (D_p/D_c) during Xianghe campaign measurements. The changes in core morphology and effective density strongly depend on their aging, which is quantified by measuring the size-resolved ambient In-BC particles with different aging degrees, as shown in Fig. 3. The shape factor of In-BC cores decreased with aging process following a power law relationship (Fig. 3a), which confirms that In-BC core transformed to more regular shape with coatings accumulation. The behavior of measured In-BC cores during the atmospheric process suggested that their morphology can reach to near sphere with strongly aging but still differs from the ideal sphere with χ of 1. The effective density of In-BC cores increased with the aging degree following an exponential function (Fig. 3b), indicating that the In-BC cores become more compact during the aging. The effective densities of In-BC cores observed in this work are significantly lower than the density of a void-free spherical BC core (1.8 $g\,cm^{-3}$), indicating that In-BC cores existed as void-contained structure in the atmosphere. For the In-BC cores observed during the campaign period, the average values of χ and ρ_{eff} are 1.2 and 1.2 $g\,cm^{-3}$ respectively, indicating In-BC cores sampled in this have a near spherical shape with internal voids. Following the Eq. (4), the average fraction of internal voids is $\sim$ 30 %. In this case, assumption of void-free sphere in previous models may have misrepresented the morphology and

density of In-BC cores in the atmosphere and induced significant uncertainties in estimating optical properties of In-BC particles.

It should be noted that presence of low-volatile coatings could induce biases in measured mobility size of In-BC cores. Low-volatile coatings remained on the surface of BC cores at 300 °C caused an overestimate of mobility size, leading to overestimates of χ and underestimates of ρ_{eff}. Figure 3 also presented the relationships between χ, ρ_{eff} and D_p/D_c ratio by assuming 5 % of BC coatings are low-volatile materials (Philippin et al., 2004). It is found that presence of 5 % low-volatile coatings can lead to $\sim$ 20 % uncertainties in average χ and ρ_{eff} calculation, and the uncertainties increased with aging process due to more accumulation of non-volatile coatings. However, the relationships between χ, ρ_{eff} and D_p/D_c are still valid.

3.3 Effects of In-BC core density on measurements of optical properties

3.3.1 D_p/D_c

Figure 4 presented the number size distribution of size-resolved In-BC particles calculated by Mie model under different assumptions of In-BC core densities. After selected by DMA1, particles still followed poly-dispersed multimodal size distribution. The first peak represents the single charged particles, which was agreed well with the prescribed size by DMA1 (200, 250, 300 or 350 nm). The second or third peak represents the distribution of multiple charged particles. To exclude the effects of multiple-charged particles, we only used single-charged particles around the first peak to investigate the shell/core ratios and absorption enhancement of In-BC particles.

As discussed in Sect. 2.2.2, evolution of core density of In-BC in the atmosphere could impact its absorption enhancement capability as the size and the refractive indices of BC core are changed during aging. Figure 5 presents the distribution of shell/core ratio (D_p/D_c) of size-resolved In-BC particles under different assumptions of core densities (1.0–1.8 $g\,cm^{-3}$) and void types (air or non-BC component). For all size ranges, higher D_p/D_c ratio are observed following the increase of In-BC core density, implying In-BC cores become more compact during aging. D_p/D_c ratio increased by ~ 25 % when In-BC core density increased from 1.0 to 1.8 g cm^{-3}. Compared to measured average In-BC core density of 1.2 g cm^{-3} during the campaign, assuming In-BC core as a void-free sphere (ρ = 1.8 g cm^{-3}) could overestimate D_p/D_c ratio by 13 %. This overestimate will then cause an inaccurate assessment on optical properties of ambient In-BC particles, which will be discussed in Sect. 3.3.2.

For the whole campaign period, the average D_p/D_c ratio ranged between 2.1–2.7 for different particle size ranges. Larger particles tend to have higher D_p/D_c ratio, indicating increased particle size and coating thickness during long range transport. D_p/D_c ratios are slightly larger for In-BC cores filled with air than for those filled with non-BC materials. For individual In-BC particle with a given volume fraction of non-BC components measured in SP2, existence of non-BC materials in the voids will decrease the coating thickness, and thereby shows a lower D_p/D_c ratio compared with internal void with air.

3.3.2 Absorption enhancement

Figure 6 presents the light absorption enhancement ratio of size-resolved In-BC particles calculated by Mie model for different core densities and void types. For ambient In-BC particles with average core density of 1.2 g cm^{-3} observed in Xianghe, the average light absorption enhanced by 1.6–1.9 times due to the atmospheric aging process. Assuming In-BC core has a void-free spherical core with density of 1.8 g cm^{-3} in the Mie model will overestimate the light absorption enhancement ratio by ~ 17 %. For polluted regions with large fraction of fresh emitted BC, current assumptions in climate models will lead to significant biases in light absorption enhancement calculation. The new approach developed in this work can estimate the absorption enhancement of ambient In-BC particles more accurately by considering impacts of In-BC core morphology and density on light absorption. In the future, climate models could be improved by including

measured morphology and density of In-BC cores when more in situ measurements for different regions are available.

Similar to the D_p/D_c ratio, absorption enhancement of In-BC particles increased with particle size due to the size growth of BC particles mainly caused by the condensation of non-BC components on the surface of BC particles. E_{ab} distribution shows one peak for observed In-BC particles at 200 nm but two peaks for particles at 250–350 nm, which can be attributed to various origins of air mass at Xianghe site. Smaller In-BC particles are mainly from local origin with less enhancement of light absorption due to weaker aging, while larger particles involve more contribution of regional transportation with stronger aging, leading to more enhancements of light absorptions. Moreover, E_{ab} is greater for In-BC core voids filled with non-BC material than that for air-filled ones, indicating that the existence of non-BC components in the core voids show a stronger capability to enhance BC absorption than allocation on the surface of BC core.

4 Conclusions

The light-absorbing capability of In-BC aerosol depends on its morphology and density, however, evolution of morphology and density of BC cores in the atmosphere are still unknown. In this study, we designed a new measurement system with VTDMA and SP2 in the purpose of measuring morphology and density of ambient In-BC cores. In the new system, size-resolved ambient In-BC particles are first selected by using both VTDMA and SP2. The mobility size and mass of In-BC cores are then measured by VTDMA and SP2 respectively and used to calculate the morphology and effective density of In-BC cores. Taking the morphology and density of ambient In-BC cores into account, our work provides a new insight into the enhancement of light absorption for In-BC particles in the atmosphere.

With the new system, we quantified the evolution in morphology and density of ambient In-BC cores with aging during an intensive field campaign in North China in 2013 summer. With the aging process, the shape factor and effective density of In-BC cores are decreased and increased respectively, indicating that In-BC cores transformed to a more regular and compact shape during aging. We found that In-BC cores hardly transform its morphology into a void-free sphere during atmospheric aging process, and thereby the effective density of most ambient In-BC cores is lower than the BC material density of 1.8 g cm^{-3}. During the campaign period, the average shape factor and effective densities of ambient In-BC cores are ~ 1.2 and ~ 1.2 g cm^{-3} respectively, implying a near-spherical shape with 30 % internal void of ambient In-BC cores.

Light absorption enhancement of ambient In-BC particles was then calculated by Mie model. Light absorption enhancement ratio was estimated to be 1.6–1.9 when using the average In-BC core density (1.2 g cm^{-3}) observed in Xianghe, ~ 15 % lower than estimates with assumption of void-free spherical structure with density of 1.8 g cm^{-3}. We can then conclude that previous models tend to overestimate the light absorption of BC particles over polluted regions where large fractions of BC are locally emitted.

With the new measurements techniques developed in this work, absorption enhancement of ambient BC particles can be more accurately with measured morphology and density of In-BC cores. To better understand the morphology and density of In-BC cores during aging process in the atmosphere, more in situ measurements in different regions should be carried out. In the future, climate models could be possibly improved by characterizing morphology and density of In-BC cores with the help of in situ measurements.

The Supplement related to this article is available online at doi:10.5194/amtd-8-12025-2015-supplement.

Acknowledgements. This study was supported by the National Natural Science Foundation of China (41222036, 21221004, 21190054 and GZ 663), and the Environmental Protection Commonweal Project of China (201409027).

References

Adler, G., Riziq, A. A., Erlick, C., and Rudich, Y.: Effect of intrinsic organic carbon on the optical properties of fresh diesel soot, P. Natl. Acad. Sci. USA, 107, 6699–6704, 2010.

Allen, M. D. and Raabe, O. G.: Slip correction measurements of spherical solid aerosol-particles in an improved millikan apparatus, Aerosol Sci. Tech., 4, 269–286, 1985.

Baumgardner, D., Popovicheva, O., Allan, J., Bernardoni, V., Cao, J., Cavalli, F., Cozic, J., Diapouli, E., Eleftheriadis, K., Genberg, P. J., Gonzalez, C., Gysel, M., John, A., Kirchstetter, T. W., Kuhlbusch, T. A. J., Laborde, M., Lack, D., Müller, T., Niessner, R., Petzold, A., Piazzalunga, A., Putaud, J. P., Schwarz, J., Sheridan, P., Subramanian, R., Swietlicki, E., Valli, G., Vecchi, R., and Viana, M.: Soot reference materials for instrument calibration and intercomparisons: a workshop summary with recommendations, Atmos. Meas. Tech., 5, 1869–1887, doi:10.5194/amt-5-1869-2012, 2012.

Bond, T. C. and Bergstrom, R. W.: Light absorption by carbonaceous particles: an investigative review, Aerosol Sci. Tech., 40, 27–67, 2006.

Bond, T. C., Habib, G., and Bergstrom, R. W.: Limitations in the enhancement of visible light absorption due to mixing state, J. Geophys. Res., 111, D20211, doi:10.1029/2006JD007315, 2006.

Cappa, C. D., Onasch, T. B., Massoli, P., Worsnop, D. R., Bates, T. S., Cross, E. S., Davidovits, P., Hakala, J., Hayden, K. L., Jobson, B. T., Kolesar, K. R., Lack, D. A., Lerner, B. M., Li, S. M., Mellon, D., Nuaaman, I., Olfert, J. S., Petaja, T., Quinn, P. K., Song, C., Subramanian, R., Williams, E. J., and Zaveri, R. A.: Radiative absorption enhancements due to the mixing state of atmospheric black carbon, Science, 337, 1078–1081, 2012.

Chan, T. W., Brook, J. R., Smallwood, G. J., and Lu, G.: Time-resolved measurements of black carbon light absorption enhancement in urban and near-urban locations of southern Ontario, Canada, Atmos. Chem. Phys., 11, 10407–10432, doi:10.5194/acp-11-10407-2011, 2011.

Cheng, Y. F., Eichler, H., Wiedensohler, A., Heintzenberg, J., Zhang, Y. H., Hu, M., Herrmann, H., Zeng, L. M., Liu, S., Gnauk, T., Brüggemann, E., and He, L. Y.: Mixing state of elemental carbon and non-light-absorbing aerosol components derived from in situ particle optical properties at Xinken in Pearl River Delta of China, J. Geophys. Res., 111, D20204, doi:10.1029/2005JD006929, 2006.

Cheng, Y., Berghof, M., Garland, R. M., Wiedensohler, A., Wehner, B., Müller, T., Su, H., Zhang, Y., Achert, P., Nowak, A., Pöschl, U., Zhu, T., Hu, M., and Zeng, L.: Influence of

soot mixing state on aerosol light absorption and single scattering albedo during air mass aging at a polluted regional site in northeastern China, J. Geophys. Res., 114, D010883, doi:10.1029/2008JD010883, 2009.
Cheng, Y. F., Su, H., Rose, D., Gunthe, S. S., Berghof, M., Wehner, B., Achtert, P., Nowak, A., Takegawa, N., Kondo, Y., Shiraiwa, M., Gong, Y. G., Shao, M., Hu, M., Zhu, T., Zhang, Y. H., Carmichael, G. R., Wiedensohler, A., Andreae, M. O., and Pöschl, U.: Size-resolved measurement of the mixing state of soot in the megacity Beijing, China: diurnal cycle, aging and parameterization, Atmos. Chem. Phys., 12, 4477–4491, doi:10.5194/acp-12-4477-2012, 2012.
DeCarlo, P. F., Slowik, J. G., Worsnop, D. R., Davidovits, P., and Jimenez, J. L.: Particle morphology and density characterization by combined mobility and aerodynamic diameter measurements, Part 1: Theory, Aerosol Sci. Tech., 38, 1185–1205, 2004.
Fuller, K. A., Malm, W. C., and Kreidenweis, S. M.: Effects of mixing on extinction by carbonaceous particles, J. Geophys. Res., 104, 15941–15954, 1999.
Gao, R. S., Schwarz, J. P., Kelly, K. K., Fahey, D. W., Watts, L. A., Thompson, T. L., Spackman, J. R., Slowik, J. G., Cross, E. S., Han, J. H., Davidovits, P., Onasch, T. B., and Worsnop, D. R. A.: Novel method for estimating light-scattering properties of soot aerosols using a modified single-particle soot photometer, Aerosol Sci. Tech., 41, 125–135, 2007.
Geller, M., Biswas, S., and Sioutas, C.: Determination of particle effective density in urban environments with a differential mobility analyzer and aerosol particle mass analyzer, Aerosol Sci. Tech., 40, 709–723, 2006.
Gysel, M., Laborde, M., Olfert, J. S., Subramanian, R., and Gröhn, A. J.: Effective density of Aquadag and fullerene soot black carbon reference materials used for SP2 calibration, Atmos. Meas. Tech., 4, 2851–2858, doi:10.5194/amt-4-2851-2011, 2011.
Jacobson, M. Z.: A physically based treatment of elemental carbon optics: implication for global direct forcing of aerosols, Geophys. Res. Lett., 27, 217–220, doi:10.1029/1999GL010968, 2000.
Jacobson, M. Z.: Strong radiative heating due to the mixing state of black carbon in atmospheric aerosol, Nature, 409, 695–697, 2001.
Khalizov, A. F., Lin, Y., Qiu, C., Guo, S., Collins, D., and Zhang, R.: Role of OH-initiated oxidation of isoprene in aging of combustion soot, Environ Sci Technol., 47, 2254–2263, 2013.

Köylü, Ü. O., Xing, Y., and Rosner, D. E.: Fractal morphology analysis of combustion-generated aggregates using angular light scattering and electron microscope images, Langmuir, 11, 4848–4854, 1995.
Knox, A., Evans, G. J., Brook, J. R., Yao, X., Jeong, C.-H., Godri, K. J., Sabaliauskas, K., and Slowik, J. G.: Mass absorption cross-section of ambient black carbon aerosol in relation to chemical age, Aerosol Sci. Tech., 43, 522–532, 2009.
Lack, D. A. and Cappa, C. D.: Impact of brown and clear carbon on light absorption enhancement, single scatter albedo and absorption wavelength dependence of black carbon, Atmos. Chem. Phys., 10, 4207–4220, doi:10.5194/acp-10-4207-2010, 2010.
Maricq, M. M. and Ning, X.: The effective density and fractal dimension of soot particles from premixed flames and motor vehicle exhaust, J. Aerosol Sci., 35, 1251–1274, 2004.
McMurry, P. H., Wang, X., Park, K., and Ehara, K.: The relationship between mass and mobility for atmospheric particles: a new technique for measuring particle density, Aerosol Sci. Tech., 36, 227–238, 2002.
Metcalf, A. R., Loza, C. L., Coggon, M. M., Craven, J. S., Jonsson, H. H., Flagan, R. C., and Seinfeld, J. H.: Secondary organic aerosol coating formation and evaporation: chamber studies using black carbon seed aerosol and the single-particle soot photometer, Aerosol Sci. Tech., 47, 326–347, 2013.
Moteki, N. and Kondo, Y.: Dependence of laser-induced incandescence on physical properties of black carbon aerosols: measurements and theoretical interpretation, Aerosol Sci. Tech., 44, 663–675, 2010.
Pagels, J., Khalizov, A. F., McMurry, P. H., and Zhang, R. Y.: Processing of Soot by Controlled Sulphuric Acid and Water Condensation Mass and Mobility Relationship, Aerosol Sci. Tech., 43, 629–640, 2009.
Park, K., Cao, F., Kittelson, D. B., and McMurry, P. H.: Relationship between particle mass and mobility for diesel exhaust particles, Environ. Sci. Technol., 37, 577–583, 2003.
Philippin, S., Wiedensohler, A., and Stratmann, F.: Measurements of non-volatile fractions of pollution aerosols with an eight-tube volatility tandem differential mobility analyzer (VTDMA-8), Aerosol Sci., 35, 185–203, 2004.
Qiu, C., Khalizov, A. F., and Zhang, R.: Soot aging from OH-initiated oxidation of toluene, Environ. Sci. Technol., 46, 9464–9472, 2012.

Discussion Paper | Discussion Paper | Discussion Paper | Discussion Paper |

Radney, J. G., You, R., Ma, X., Conny, J., Hodges, J. T., Zachariah, M. R., Hodges, J. T., and Zangmeister, C. D.: Dependence of soot optical properties on particle morphology: measurements and model comparisons, Environ. Sci. Technol., 48, 3169–3176, 2014.

Rissler, J., Messing, M. E., Malik, A. I., Nilsson, P. T., Nordin, E. Z., Bohgard, M., Sanati, M., and Pagels, J. H.: Effective density characterization of soot agglomerates from various sources and comparison to aggregation theory, Aerosol Sci. Tech., 47, 792–805, 2013.

Rissler, J., Nordin, E. Z., Eriksson, A. C., Nilsson, P. T., Frosch, M., Sporre, M. K., Wierzbicka, A., Svenningsson, B., Löndahl, J., Messing, M. E., Sjogren, S., Hemmingsen, J. G., Loft, S., Pagels, J. P., and Swietlicki, E.: Effective density and mixing state of aerosol particles in a near-traffic urban environment, Env. Sci. Technol., 48, 6300–6308, 2014.

Scarnato, B. V., Vahidinia, S., Richard, D. T., and Kirchstetter, T. W.: Effects of internal mixing and aggregate morphology on optical properties of black carbon using a discrete dipole approximation model, Atmos. Chem. Phys., 13, 5089–5101, doi:10.5194/acp-13-5089-2013, 2013.

Schwarz, J. P., Gao, R. S., Fahey, D. W., Thomson, D. S., Watts, L. A., Wilson, J. C., Reeves, J. M., Darbeheshti, M., Baumgardner, D. G., Kok, G. L., Chung, S. H., Schulz, M., Hendricks, J., Lauer, A., Kärcher, B., Slowik, J. G., Rosenlof, K. H., Thompson, T. L., Langford, A. O., Loewenstein, M., and Aikin, K. C.: Single-particle measurements of midlatitude black carbon and light-scattering aerosols from the boundary layer to the lower stratosphere, J. Geophys. Res.-Atmos., 111, D16207, doi:10.1029/2006JD007076, 2006.

Sedlacek, A. J., Lewis, E. R., Kleinman, L., Xu, J., and Zhang, Q.: Determination of and evidence for non-core-shell structure of particles containing black carbon using the Single-Particle Soot Photometer (SP2), Geophys. Res. Lett., 39, L050905, doi:10.1029/2012GL050905, 2012.

Sgro, L. A., Basile, G., Barone, A. C., D'Anna, A., Minutolo, P., Borghese, A., and D'Alessio, A.: Detection of combustion formed nanoparticles, Chemosphere, 51, 1079–1090, 2003.

Slowik, J. G., Stainken, K., Davidovits, P., Williams, L. R., Jayne, J. T., Kolb, C. E., Worsnop, D. R., Rudich, Y., DeCarlo, P. F., and Jimenez, J. L.: Particle morphology and density characterization by combined mobility and aerodynamic diameter measurements. Part 2: Application to combustion-generated soot aerosols as a function of fuel equivalence ratio, Aerosol Sci. Tech., 38, 1206–1222, 2004.

Tuch, T. M., Haudek, A., Müller, T., Nowak, A., Wex, H., and Wiedensohler, A.: Design and performance of an automatic regenerating adsorption aerosol dryer for continuous operation at monitoring sites, Atmos. Meas. Tech., 2, 417–422, doi:10.5194/amt-2-417-2009, 2009.

Wehner, B., Berghof, M., Cheng, Y. F., Achtert, P., Birmili, W., Nowak, A., Wiedensohler, A., Garland, R. M., Pöschl, U., Hu, M., and Zhu, T.: Mixing state of nonvolatile aerosol particle fractions and comparison with light absorption in the polluted Beijing region, J. Geophys. Res., 114, D010923, doi:10.1029/2008JD010923, 2009.

Xue, H., Khalizov, A. F., Wang, L., Zheng, J., and Zhang, R.: Effects of dicarboxylic acid coating on the optical properties of soot, Phys. Chem. Chem. Phys., 11, 7869–7875, 2009a.

Xue, H. X., Khalizov, A. F., Wang, L., Zheng, J., and Zhang, R. Y.: Effects of coating of dicarboxylic acids on the mass-mobility relationship of soot particles, Environ. Sci. Technol., 43, 2787–2792, 2009b.

Zhang, R., Khalizov, A. F., Pagels, J., Zhang, D., Xue, H., and McMurry, P. H.: Variability in morphology, hygroscopicity, and optical properties of soot aerosols during atmospheric processing, P. Natl. Acad. Sci. USA., 105, 10291–10296, 2008.

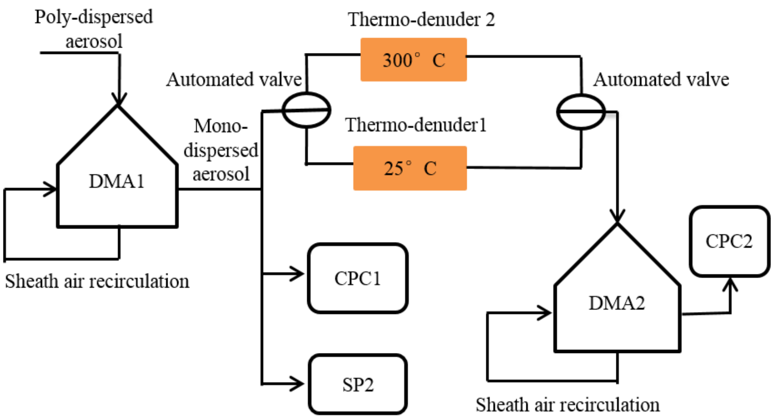

Figure 1. Schematic of instrument setup.

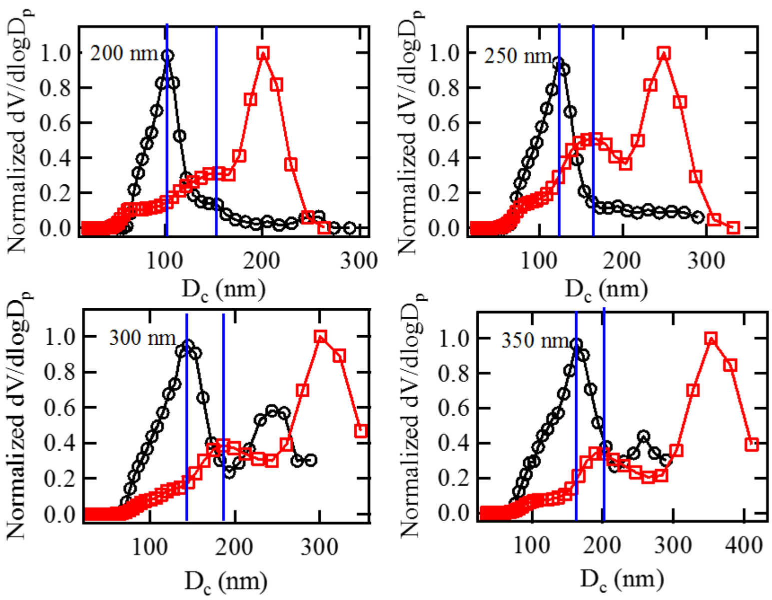

Figure 2. Normalized volume size distribution of the In-BC cores from SP2 measurements (black marks and line) and the residual particles from VTDMA measurements at 300 °C (red marks and line); before measurements of SP2 and heating at 300 °C, the initial particle size selected by DMA1 are 200, 250, 300 and 350 nm, respectively; the blue lines represent the In-BC core size at peaks of volume size distribution from VTDMA and SP2 measurement.

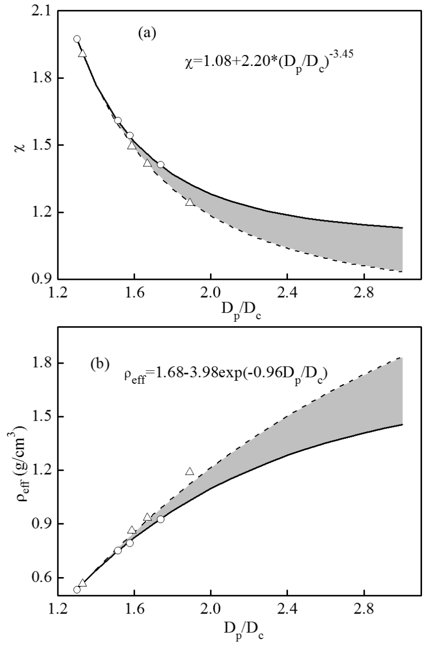

Figure 3. Changes in χ **(a)** and ρ_{eff} **(b)** of In-BC cores undergoing aging. The solid lines are fitted based on the data (circle markers) calculated by the measured peak values for size-resolved In-BC particles shown in Fig. 2; the dash lines are fitted based on the data (triangle markers) derived from the assumption of 5 % non-volatile coating fraction; the grey shaded area represented the uncertainty of morphology and density of In-BC cores obtained from our study.

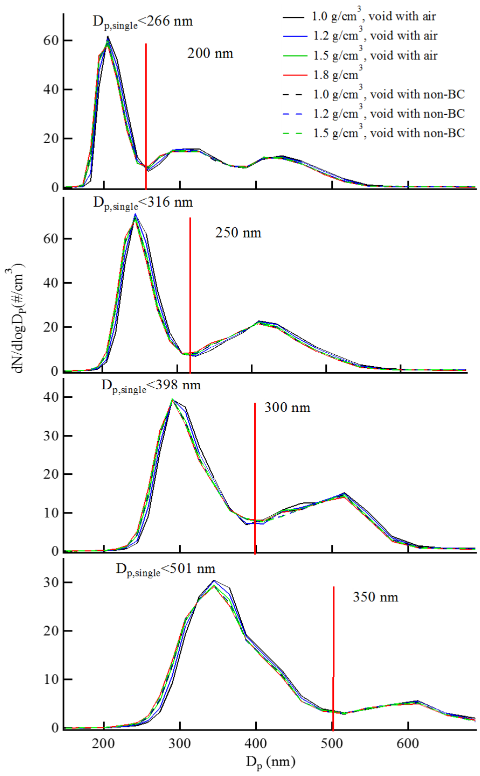

Figure 4. The number size distribution of size-resolved ambient In-BC particles with different core densities and void types.

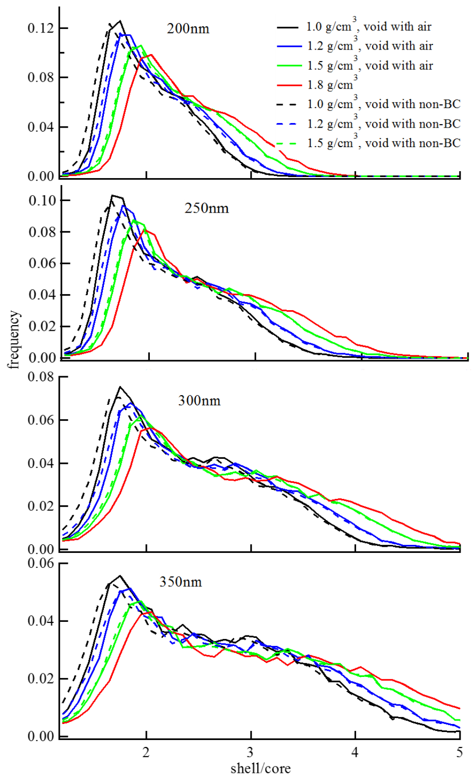

Figure 5. The shell / core (D_p/D_c) ratios of size-resolved ambient In-BC particles with different core densities and void types.

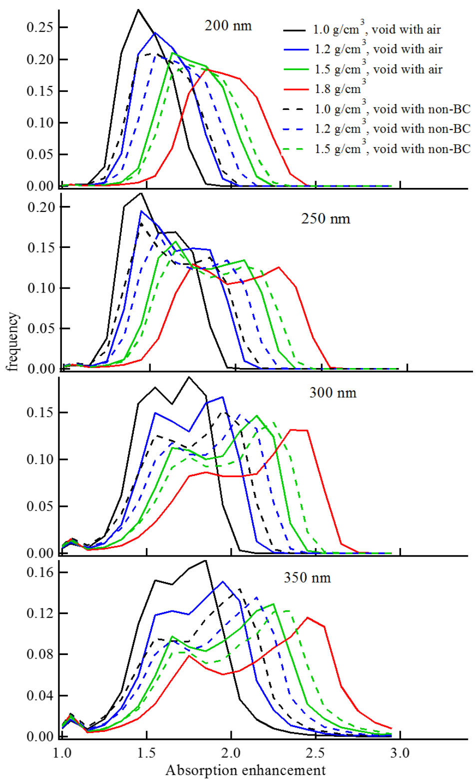

Figure 6. Absorption enhancement of size-resolved ambient In-BC particles with different core densities and void types.

Discussion Paper | Discussion Paper | Discussion Paper | Discussion Paper |